Coherent incident field information through thick random scattering media from speckle correlations over source position

Zhenyu Wang, Kevin J. Webb,* and Andrew M. Weiner

School of Electrical and Computer Engineering, Purdue University, West Lafayette, Indiana 47907, USA

*Corresponding author: webb@purdue.edu

Received 2 March 2010; accepted 20 August 2010;
posted 14 September 2010 (Doc. ID 124918); published 18 October 2010

With two nonoverlapping beams incident at different angles on a heavily scattering medium, the spatial correlation of speckle patterns over source position has a beat that is related to the incident angle difference. A model presented explains the measurement. The spatial correlation is shown to decorrelate faster than the beam intensity correlation function and to be sensitive to the incident field profile. Increased scatter results in more rapid decorrelation. This work suggests new opportunities for imaging through scattering media. © 2010 Optical Society of America

OCIS codes: 030.6600, 030.6140, 110.6150, 290.7050.

1. Introduction

Imaging and communicating through scattering media are fundamental to a variety of biological and environmental problems. While the magnitude and phase of light scattered by a disordered medium are randomized, all information about coherent incident light is not lost. There is a relationship between the incident and transmitted wave vectors that diminishes with increasing scatter, causing a speckle pattern to shift slightly according to small changes in the incident beam angle [1,2], the so-called "memory effect." This phenomenon diminishes exponentially with increasing scattering medium thickness and, hence, is measurable only with weak scatter. Short-range correlations (on the wavelength scale) of scattered microwave signals have been described [3]. Enhanced backscattering occurs due to the weak localization of light, and this is a time reversal memory effect, where light is preferentially scattered back along the incident wave vector direction [4,5], dependent on polarization [6]. It has also been demonstrated that one can focus light to some degree by controlling the spatially dependent incident field [7].

Here, we demonstrate that it is possible to access the incident field spatial correlation, and with locally planar phase fronts, the incident angle difference between two beams. We describe experiments that show how a spatial correlation of speckle over scanned source position depends on the support of the incident beam and the scattering properties of the random medium. With two beams incident at fixed and different angles, this spatial correlation as a function of the position of the jointly scanned beams is sensitive to the angular difference. Importantly, this effect occurs even for thick, highly scattering material, making it distinct from the memory effect [1,2]. Figure 1 shows a schematic of the measurements we performed. As the single input beam is scanned, a correlation between the speckle intensity patterns at the imaging point on the right, with the beam at two positions separated by Δx, reduces with increasing Δx and depends on both the beam and the degree of scatter. With two spatially separated incident beams having incident angle differences that are fixed with scan position Δx, we find a coherent oscillation in the intensity correlation over position that is dictated by this angle. To emphasize the

0003-6935/10/305899-07$15.00/0

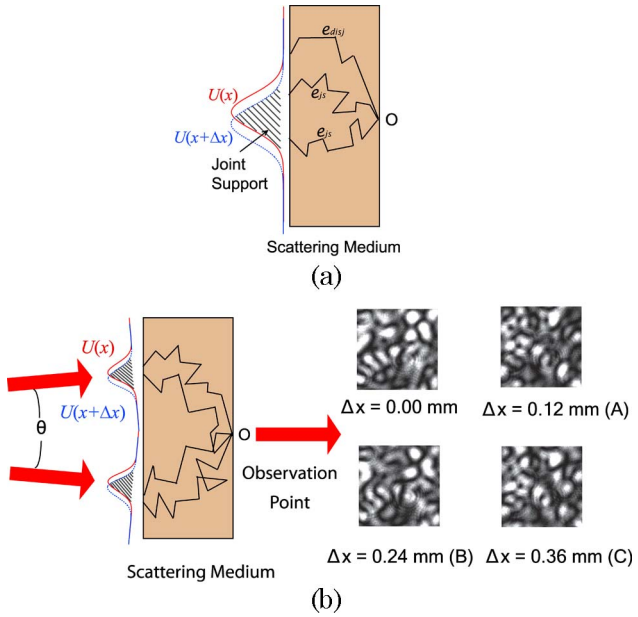

Fig. 1. (Color online) (a) Scanned input beam arrangement, showing the joint support that contributes to the intensity correlation at a detector point on the right side of the scattering medium, and the disjoint region, which does not. $U(x)$ is the incident field and $U(x+\Delta x)$ is the same field translated by Δx. (b) Two spatially separated input beams, with different incident angles, produce a beat in the measured intensity correlation as a function of Δx. The four speckle patterns correspond to a portion of the image for the measurement of Fig. 3(a): upper left, reference position; upper right, decorrelated result (Point A in Fig. 3(a)]; lower left, second correlation peak (Point B in Fig. 3(a)]; lower right, second decorrelated valley (Point C in Fig. 3(a)]. The $\Delta x = 0$ and $\Delta x = 0.24$ mm patterns are virtually identical.

partial recovery of the coherent speckle information with the scan position of the two beams, note the similarity of the top and bottom speckle patterns on the left in Fig. 1, corresponding to adjacent correlation peaks, and the decorrelated patterns on the right.

2. Experiments

Figure 2 shows our two-beam experiment. The laser source used was a tunable (over 80 GHz) external cavity (Littman–Metcalf design) laser diode (New Focus Vortex 6017), with a single-mode output and a linewidth of approximately 5 MHz. The light source had a center wavelength at about 850 nm and an average power of 10 mW. An isolator was used to prevent backreflections entering the laser. The two beams were created by a 50∶50 beam splitter and mirrors M1 and M2. The location (source position) of the linearly polarized input beam was controlled by mirror M3, which was mounted on a translation stage. We denote the center-to-center beam separation at the left surface of the scattering sample as d and the distance from M2 to the left face of the scattering medium along a line that bisects the angle between the two beams as D. For the single-beam experiments, the beam reflected from mirror M2 (shown as a dashed line in Fig. 2) was removed. A speckle pattern was formed by imaging light transmitted through the scattering sample with a CCD camera, then only the incident light was scanned in space, and another speckle pattern collected. In all cases, the sample itself and the CCD camera were kept fixed. This process was continued to provide speckle pattern data that were used to form spatial correlations. The spatial filter controls the speckle size for satisfactory imaging and the polarizer selects the polarization state imaged by the camera. A 0.7 mm × 0.9 mm spot on the right (transmission) side of the scattering sample was imaged with a magnification of 10 onto the CCD camera. The imaged

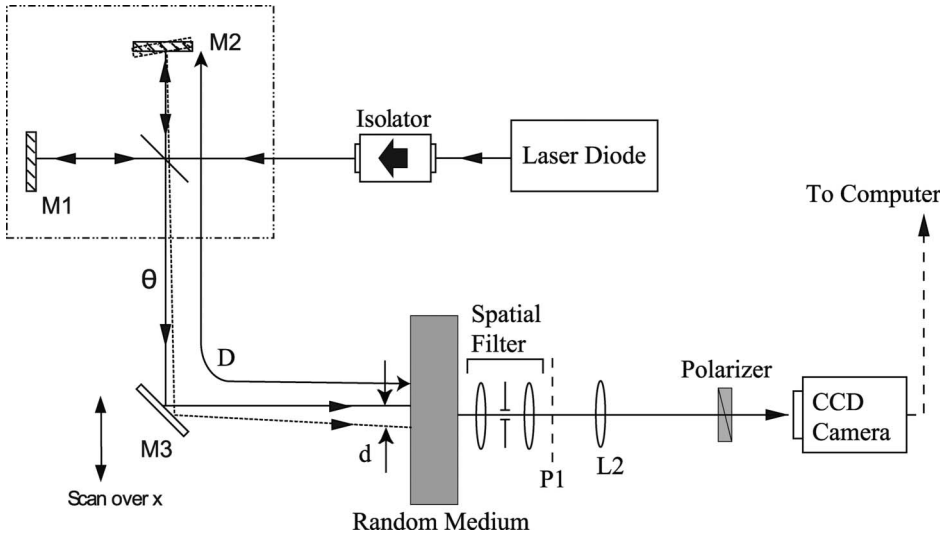

Fig. 2. Experimental setup for the correlation over source position with two beams from an 850 nm laser. The distance between M2 and the left surface of the scattering medium is D (1422, 1118, and 934 mm used), the center-to-center distance between the beams at this surface is d (6.86 and 4.71 mm, for example), and the angle between the beams is θ. In the single-beam experiments, the dashed beam was removed. The unrestricted beam had a FWHM of about 1 mm. The spatial filter controls the speckle size and L2 images a small spot on the right surface of the scattering medium onto the CCD camera. A small region on the right side of the scattering medium is imaged to P1 and then magnified by L2 for imaging at the CCD camera. The "Scan over x" results in Δx.

speckle size was large enough relative to the CCD camera pixel size to allow good resolution. Statistics were obtained from a constant mean speckle pattern (over the small imaging spot) that provided an adequate number of independent samples (which is equivalent to random rearrangement of the random scatters and measurement at a single point in space). At the left surface of the scattering medium, the laser had a 1 mm FWHM intensity spot. The scattering samples used in the experiment were commercial white acrylics (Cyro Industries, Acrylite FF) with TiO_2 particles of average diameter approximately 50 nm.

First, consider the case where a single incident laser beam was scanned. Referring to Fig. 2, the scan was achieved by moving mirror M3 linearly, with the scattering medium and detector fixed, and linear copolarized light (the same as the incident field) was measured. We collected speckle patterns at a fixed position on the right side of the scattering sample as a function of scan position, thereby forming the normalized spatial correlation $\langle \tilde{I}[U(x)]\tilde{I}[U(x+\Delta x)]\rangle$ between the speckle pattern with incident field $U(x)$ and that with a displaced beam $U(x+\Delta x)$, as a function of scan position Δx, where $\tilde{I}(\cdot) = (I(\cdot) - \langle I(\cdot)\rangle)/\langle I(\cdot)\rangle$ is the normalized intensity and $\langle\cdot\rangle$ is the statistical average. Here, $U(x)$ refers to the spatial profile of the input field, and Δx is the displacement of the input beam (on the left side of scattering medium). I is the speckle intensity pattern observed at the CCD plane. Our normalized spatial correlation quantifies the resemblance between speckle patterns recorded on the right side of the scattering sample as a function of input beam displacement Δx on the left side. The incident beam and the detector spot were axially aligned when $\Delta x = 0$. Example data are shown as the envelopes in Figs. 3(a) and 3(b).

Using the two-beam arrangement of Fig. 2, we performed intensity correlations of the unrestricted laser beams over source position, with the two beams having fixed separation d when scanned, i.e., fixed angular difference, again with copolarized light. In all cases, the beam separation d was large compared to the individual beam sizes, i.e., the two beams were nonoverlapping. The beam splitter and two mirrors in Fig. 2 created two identical beams having different incident angles. As M3 was scanned, thereby varying Δx, there was a negligible change in D (on the scale of the data we present). Figures 3(a) and 3(b) show our results with the same d and D, but different scattering sample thicknesses (the case in Fig. 3(b) is more scattering), and Fig. 3(c) has fixed D and varying d. The scattering samples had a reduced scattering coefficient (from a diffusion model with the domain sufficiently thick) of $\mu_s' = 4\ \mathrm{cm}^{-1}$. As the samples had negligible absorptive loss, the transport mean free path (for photon direction randomization) becomes $l^* = 1/\mu_s' = 2.5$ mm. Notice that the single-beam result forms the envelope for the ripple in the two-beam case. In all cases, the ripple period

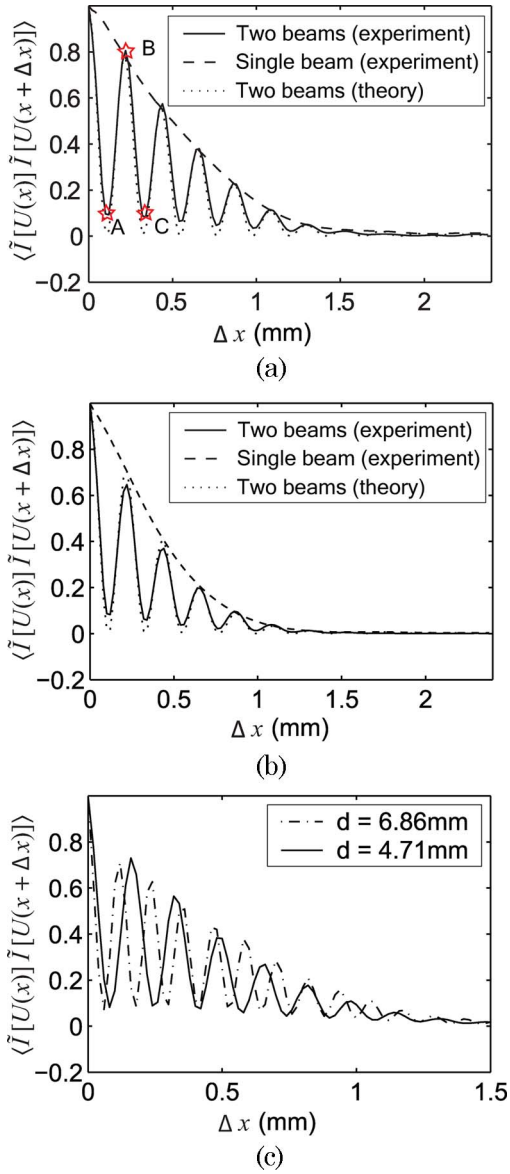

Fig. 3. (Color online) Spatial correlation for two incident beams with an angular difference: referring to Fig. 2, $D = 1118$ mm, $d = 4.32$ mm, and a thickness of (a) 9 mm and (b) 12 mm; (c) $D = 934$ mm, with $d = 6.86$ mm and $d = 4.71$ mm, and a 9 mm sample thickness. The unrestricted beam had a FWHM of about 1 mm, and $\mu_s' = 4\ \mathrm{cm}^{-1}$. The labels A, B, and C indicate points where the speckle patterns of Fig. 1(b) were captured.

is given by $\Lambda = \lambda D/d = \lambda/\theta$, where θ is the angular difference between the two incident beams and λ is the vacuum wavelength of the light. The dotted line [in Figs. 3(a) and 3(b)] is the result with a model comprised of the measured single-beam spatial correlation, as an envelope, and a sinusoidal ripple having period $\Lambda = \lambda D/d$, and this shows excellent agreement. To confirm this understanding of the basis for the ripple in the spatial correlation, Fig. 4(a) shows the measured Λ as a function of λ/d for three D values. For each D, all data can be fit to a straight line having slope D. Figure 4(b) plots the measured Λ as a function of λ/θ, clearly showing the linear relationship and establishing that we have

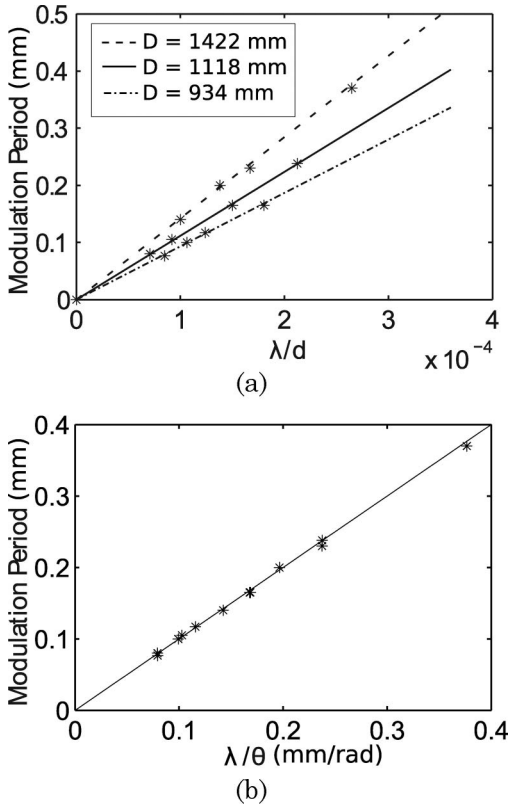

Fig. 4. (a) Measured modulation period as a function of λ/d and for different D (points) and straight line fits. (b) Measured modulation period as a function of λ/θ (points) and the predicted value (solid line).

sensitivity to the difference in incident wave vector for the two beams. The sinusoidal beating remains even for heavy scatter (with a period that is independent of the scatter).

To determine whether the speckle patterns were shifting or randomizing as a result of input beam scan, we performed a spatial cross correlation (over the speckle pattern coordinates) between the speckle patterns $\tilde{I}[U(x)]$ and $\tilde{I}[U(x+\Delta x)]$. We found that the peak spatial cross correlation was at zero spatial shift, indicating that the speckle pattern was not moving as the beam scanned. Therefore, the decorrelation that we find is due to randomization of the speckle pattern. Consequently, there is no translation in the speckle patterns shown in Fig. 1(b).

We investigated spatial correlations using a single beam illuminating one or two circular apertures. Figure 5(a) shows results for varying single apertures of diameter a. The scattering medium was of thickness 9 mm and had $\mu_s' = 4\ \mathrm{cm}^{-1}$. In general, we expect the speckle pattern to decorrelate when the incident field moves away from its original position, leading to a reduction in intensity correlation with increasing Δx. Figure 5(a) shows that decreasing the aperture size results in a more rapid decorrelation. For reference, we have also plotted the calculated beam intensity autocorrelation function for each aperture, assuming uniform intensity within the aperture, in Fig. 5(a). Scatter results in a more rapid decorrelation, relative to the beam autocorrelation. Figure 5(b) shows measured correlation data for two circular apertures, in comparison with a single aperture. Notice the peak in the double aperture case at 0.5 mm, corresponding to the aperture separation. Correlations over source position thus provide information on source location and support. Note that the small separation between the two apertures allows the satellite correlation peak to be observed in Fig. 5(b), while the large separation between the unrestricted beams in Fig. 3, relative to the Δx distance scale plotted, does not produce a peak due to one beam overlapping the other, as the two beams are scanned.

With a single unrestricted beam, we measured speckle intensity patterns at each source scan position using samples having $\mu_s' = 4\ \mathrm{cm}^{-1}$ and $\mu_s' = 14\ \mathrm{cm}^{-1}$ and various thicknesses. The measured correlations over source position are shown in Fig. 6. Figure 6(a) gives the linear copolarized (Co-pol) and cross-polarized (Cross-pol) correlations for various thicknesses with $\mu_s' = 4\ \mathrm{cm}^{-1}$. Increasing scatter forces a more rapid decorrelation. This is confirmed in Fig. 6(b), where the thickness is fixed at either 6 or 12 mm but the samples had different scattering coefficients (the larger μ_s' is, the more scattering and,

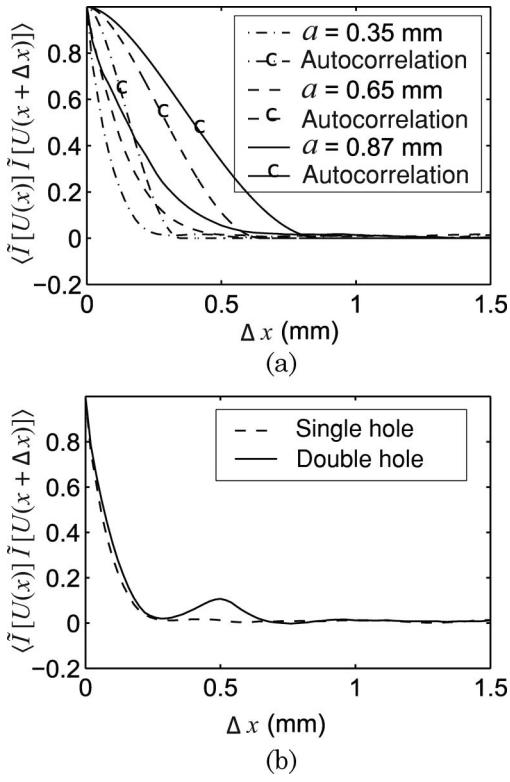

Fig. 5. (a) Spatial speckle correlation over source position for illumination through a circular aperture of varying size. For reference, the calculated aperture/beam autocorrelation function is plotted. (b) Comparison of a single circular aperture of diameter 0.35 mm and two apertures of this size with a 0.5 mm center-to-center distance. The scattering sample was 9 mm thick and had $\mu_s' = 4\ \mathrm{cm}^{-1}$.

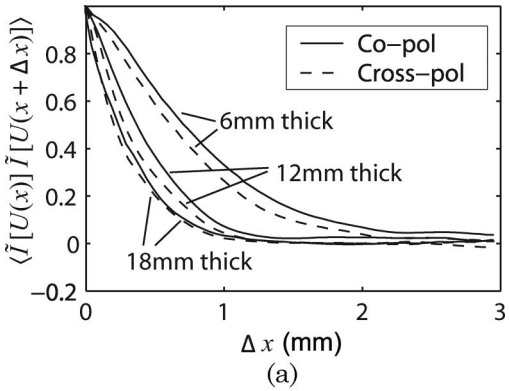

(a)

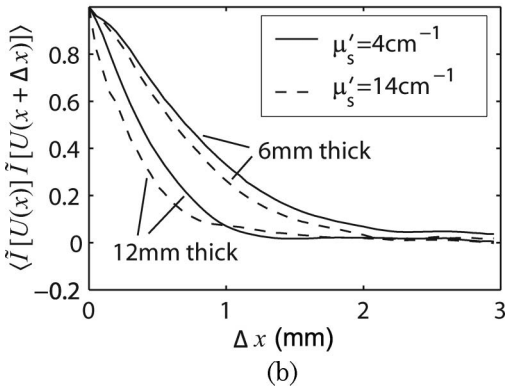

(b)

Fig. 6. (a) Spatial correlation over the source coordinate for linear co- and cross-polarized light and various sample thicknesses for a scattering sample with $\mu_s' = 4$ cm^{-1}. (b) Copolarized intensity correlation for samples having $\mu_s' = 4$ cm^{-1} and $\mu_s' = 14$ cm^{-1} and thicknesses of 6 and 12 mm.

hence, the shorter transport length). More rapid decorrelation occurs with both increasing sample thickness and increasing μ_s'. It is also interesting to note that Fig. 6(a) indicates that the intensity correlation for cross-polarized light decorrelates faster than for copolarized light. The cross-polarized light tends to be more heavily scattered, as we showed before in frequency correlations [8], and that result is again consistent with more rapid spatial decorrelation with increasing scatter. This difference between copolarized light and cross-polarized light for the same scattering medium diminishes as the amount of scatter increases.

3. Theory

For circular Gaussian fields [9], the moment theorem of Reed allows fourth-order field moments to be written in terms of second-order moments as [10]

$$\langle \tilde{I}[U(\mathbf{r})]\tilde{I}[U(\mathbf{r}+\Delta\mathbf{r})]\rangle = |\langle \tilde{E}[U(\mathbf{r})]\tilde{E}^*[U(\mathbf{r}+\Delta\mathbf{r})]\rangle|^2, \quad (1)$$

where $\tilde{I}[U(\mathbf{r})] = |\tilde{E}[U(\mathbf{r})]|^2$ is the normalized intensity at a point $\mathbf{r_d}$ on the right surface of the scattering sample with an input beam $U(\mathbf{r})$ on the left face (the transmission arrangement of Fig. 2), and the right hand side is the magnitude squared of the mutual coherence function [11]. As the detector point is assumed fixed in this representation (with statistics generated from random arrangement of the scatterers) and the source points vary in space, we choose a notation where spatial arguments apply to the incident fields. The field correlation with respect to the input field scan position $\Delta\mathbf{r}$ can be written as follows:

$$\langle \tilde{E}[U(\mathbf{r})]\tilde{E}^*[U(\mathbf{r}+\Delta\mathbf{r})]\rangle = \left\langle \int_{\mathbf{r}'} d\mathbf{r}' G(\mathbf{r}_d,\mathbf{r}')U(\mathbf{r}') \int_{\mathbf{r}''} d\mathbf{r}'' \times G^*(\mathbf{r}_d,\mathbf{r}'')U^*(\mathbf{r}''+\Delta\mathbf{r})\right\rangle, \quad (2)$$

where $U(\cdot)$ is the incident field on the left of the scattering slab and $G(\mathbf{r_d},\cdot)$ is the electric field Green's function. The average in Eq. (2) has contributions when photons have correlated paths, and assuming that this occurs when there is an intersecting source support, as the beam is scanned from $\mathbf{r}$ to $\mathbf{r}+\Delta\mathbf{r}$, Eq. (2) becomes

$$\langle \tilde{E}[U(\mathbf{r})]\tilde{E}^*[U(\mathbf{r}+\Delta\mathbf{r})]\rangle = \int_{js} d\mathbf{r}' U(\mathbf{r}')U^*(\mathbf{r}'+\Delta\mathbf{r}) \times \langle |G(\mathbf{r}_d,\mathbf{r}')|^2\rangle, \quad (3)$$

where js is the joint support between the beam in position $\mathbf{r}$ and $\mathbf{r}+\Delta\mathbf{r}$.

Suppose now that the input beam has the form $U(\mathbf{r}) = U_0(\mathbf{r})e^{i\mathbf{k}\cdot\mathbf{r}}$, where $U_0(\mathbf{r})$ is an amplitude function and $\mathbf{k}$ is the wave vector, i.e., that the incident beam is a local plane wave. Let the incident wave vector have a component $\mathbf{k}_\parallel$ parallel to the surface of the planar scattering medium. We can rewrite Eq. (3) as

$$\begin{aligned}\langle \tilde{E}[U(\mathbf{r})]\tilde{E}^*[U(\mathbf{r}+\Delta\mathbf{r})]\rangle &= e^{-i\mathbf{k}_\parallel\cdot\Delta\mathbf{r}} \int d\mathbf{r}' U_0(\mathbf{r}')U_0^*(\mathbf{r}'+\Delta\mathbf{r}) \times \langle |G(\mathbf{r}_d,\mathbf{r}')|^2\rangle \\ &= e^{-i\mathbf{k}_\parallel\cdot\Delta\mathbf{r}}P(\Delta\mathbf{r}), \end{aligned} \quad (4)$$

where $P(\Delta\mathbf{r})$ is a function of the incident field (support) and the scatter, and the exponential describes the phase front of the incident field.

Obviously, the phase term in Eq. (4) is lost in the one-beam intensity correlation, where $|\langle \tilde{E}[U(\mathbf{r})]\tilde{E}^*[U(\mathbf{r}+\Delta\mathbf{r})]\rangle|^2 = |P(\Delta\mathbf{r})|^2$. However, consider the case of two nonoverlapping beams with $\tilde{U} = (\tilde{U}_1 + \tilde{U}_2)/\sqrt{2}$, which results in $\tilde{E} = (\tilde{E}_1 + \tilde{E}_2)/\sqrt{2}$, where $\tilde{E}_i$ $(i = 1, 2)$ is the field at $\mathbf{r}_d$ due to beam i having incident field U_i. Mapping to our experimental case of scanning in the x direction, $\mathbf{r} = x\hat{x}$ and $\Delta\mathbf{r} = \Delta x\hat{x}$, and the second-order field moment becomes (in one dimension)

$$\langle \tilde{E}[U(x)]\tilde{E}^*[U(x+\Delta x)]\rangle = \frac{1}{2}\langle(\tilde{E}_1[U_1(x)] + \tilde{E}_2[U_2(x)]) \times (\tilde{E}_1^*[U_1(x+\Delta x)] + \tilde{E}_2^*[U_2(x+\Delta x)])\rangle = \frac{1}{2}\{\langle \tilde{E}_1[U_1(x)]\tilde{E}_1^*[U_1(x+\Delta x)]\rangle + \langle \tilde{E}_2[U_2(x)] \times \tilde{E}_2^*[U_2(x+\Delta x)]\rangle\}, \quad (5)$$

where the beam separation d is assumed large enough to neglect the cross terms. We consider $\mathbf{k}_\parallel = k_x\hat{x}$. For the case of identical beams having differing incident angles, from Eq. (5) and using Eq. (4),

$$|\langle \tilde{E}[U(x)]\tilde{E}^*[U(x+\Delta x)]\rangle|^2 = \frac{1}{4}|P(\Delta x)|^2|e^{-ik_{x1}\Delta x} + e^{-ik_{x2}\Delta x}|^2 = |P(\Delta x)|^2 \times \frac{[1+\cos(\Delta k_x \Delta x)]}{2}, \quad (6)$$

where $\Delta k_x = k_{x1} - k_{x2}$ and the normalization gives $P(0) = 1$. Equation (6) describes the envelope through $|P(\Delta x)|^2$, and the ripple period of the measured data in Fig. 3 when one identifies $\sin\theta \approx \theta = \Delta k_x \lambda/(2\pi) = \lambda/\Lambda$, or $\Lambda = \lambda/\theta$. It is quite remarkable that information about Δk_x is retained in the correlation $\langle \tilde{I}[U(x)]\tilde{I}[U(x+\Delta x)]\rangle$.

4. Discussion

Phase front information is retained in the scattered speckle pattern and available from an intensity correlation over incident field position with a simultaneously moving object and reference. One may anticipate that spatial correlations over incident field position will retain information about spatial frequency spectra for fields with a distribution of $\mathbf{k}_\parallel$ in one dimension or two dimensions. Our work, therefore, may form the basis of a new approach to capture improved image information through heavily scattering media.

Scanning the incident field in Δx, with a single beam obliquely incident on the scattering sample, produces a linear phase progression in the field at each point within the beam. However, the intensity correlation over incident field position in Eq. (1) is not sensitive to this phase modulation. Introducing the second beam, as a reference with known phase front information, allows information on the phase front of the signal beam to be determined, as is clear from Eq. (4). Note that the phase at each point within each beam is being modulated as the incident field is scanned, as in the single-beam case, but now angle or phase front information is available. Also, as Eq. (4) shows, information about the scattering medium and the incident field is contained within $P(\Delta\mathbf{r})$.

The model result in Fig. 3 uses the single-beam correlation to determine $|P(\Delta x)|$, and the known incident beam angles to arrive at Δk_x, referring to Eq. (6). The degree to which the two beams were partial plane waves with uniform phase fronts limits the nulls in the experimental data, i.e., we attribute the nonzero nulls in Figs. 3(a) and 3(b) to slightly nonplanar phase fronts in the unrestricted beams. In general, the model fits the data quite nicely.

Further insight can be gained by considering uniform plane wave illumination of the scattering medium, i.e., $P(\Delta\mathbf{r}) = 1$. With single plane wave illumination, the intensity correlation over scan position of this field is constant. With two plane waves incident at different angles, and imaging the speckle in a small spot, the intensity correlation over scan position (of both or just one beam, in this case) will be sinusoidal, because the incident field at each point in space is periodic and there is a reference. Without a spatial scan, but by scanning the phase of one plane wave relative to the other, the incident field and, hence, the speckle pattern will also be periodic. The phase adjustment could also be done with both waves incident at the same angle, and the speckle pattern would remain periodic in the control phase. The important distinction between scanning the incident field over position and phase is that the former gives rise to phase front information, which appears not to have been recognized previously.

In contrast to the spatial correlation with respect to source position that we have described, correlations over position in the detector plane can also provide important information. For instance, the autocorrelation of a given speckle pattern is a useful measure of speckle size, and this result is dictated by the spatial filter aperture in Fig. 2 and is independent of the particular incident field in our imaging arrangement. The spatial correlation results presented throughout this paper are independent of the speckle size, as controlled by the imaging optics. Another example is the van Cittert–Zernike theorem, which relates the far-field mutual intensity in a detector plane (between image plane spatial points) to the intensity in a source plane (which in our case would be the random intensity on the image side of the scattering medium, if measurements had been made in that regime), through a Fourier transform [9]. Yet another example is the work on field correlations over wave vector on the transmission side (or position in the detection plane), which has been presented as a generalization of the memory effect [12].

It is also interesting to draw an analogy with our previous work [13], where the path length difference of two incident beams was retrieved from a correlation of speckle patterns as the laser frequency was scanned. In that experiment, we found $\langle \tilde{I}(\omega)\tilde{I}(\omega+\Delta\omega)\rangle = |P(\Delta\omega)|^2[1+\cos(\Delta\omega\Delta t)]/2$, with Δt the delay of one input beam relative to the other and $\Delta\omega$ the offset in the laser circular frequency, which has the same mathematical form as Eq. (6).

5. Conclusions

We have shown that information about the angular difference between two nonoverlapping beams incident on a random scattering medium can be successfully retrieved from the spatial correlation function over excitation position. The envelope is governed by the single-beam case, which is a function of the source and the amount of scatter. Interestingly, the beat due to the incident angle difference is not a function of the amount of scatter and is, therefore, a long-range effect. This observation should be useful in various applications involving imaging through and within scattering media.

This work was supported by the National Science Foundation (NSF) under grants 0203240-ECS, 0323037-ECS, and 0701749-ECCS.

References

1. S. Feng, C. Kane, P. A. Lee, and A. D. Stone, "Correlations and fluctuations of coherent wave transmissions through disordered media," Phys. Rev. Lett. **61**, 834–837 (1988).
2. I. Freund, M. Rosenbluh, and S. Feng, "Memory effects in propagation of optical waves through disordered media," Phys. Rev. Lett. **61**, 2328–2331 (1988).
3. P. Sebbah, B. Hu, A. Z. Genack, R. Pnini, and B. Shapiro, "Spatial-field correlation: the building block of mesoscopic fluctutations," Phys. Rev. Lett. **88**, 123901 (2002).
4. P.-E. Wolf and G. Maret, "Weak localization and coherent backscattering of photons in disordered media," Phys. Rev. Lett. **55**, 2696–2699 (1985).
5. R. Berkovits and M. Kaveh, "Time-reversed memory effects," Phys. Rev. B **41**, 2635–2638 (1990).
6. R. Berkovits and M. Kaveh, "The vector memory effect for waves," Europhys. Lett. **13**, 97–101 (1990).
7. I. M. Vellekoop and A. P. Mosk, "Focusing coherent light through opaque strongly scattering media," Opt. Lett. **32**, 2309–2311 (2007).
8. Z. Wang, M. A. Webster, A. M. Weiner, and K. J. Webb, "Polarized temporal impulse response for scattering media from third-order frequency correlations of speckle intensity patterns," J. Opt. Soc. Am. A **23**, 3045–3053 (2006).
9. J. Goodman, *Statistical Optics* (Wiley, 1985).
10. I. S. Reed, "On a moment theorem for complex Gaussian processes," IRE Trans. Inf. Theory **8**, 194–195 (1962).
11. L. Mandel and E. Wolf, *Optical Coherence and Quantum Optics* (Cambridge U. Press, 1995).
12. I. Freund, "Looking through walls and around corners," Physica A (Amsterdam) **168**, 49–65 (1990).
13. Z. Wang, A. M. Weiner, and K. J. Webb, "Interferometry from a scattering medium," Opt. Lett. **32**, 2013–2015 (2007).